Docking Method for a Wheelchair and a care Robot Using Both Teleoperation and Autonomous Control

Hidetoshi Ikeda, Nobuyuki Yamashima, and Shogo Haruta
Department of Mechanical Engineering, National Institute of Technology,
Toyama College, Toyama, Japan
Email: ikedah@nc-toyama.ac.jp

Eiji Nakano
Robofesta Org., Tsukuba, Japan
Email: nakanoeini@gmail.com

***Abstract*—This paper describes a docking method for cooperative step climbing for a wheelchair and a care robot which has individually driven wheels. The robot is moved by autonomous control or teleoperation, and the robot operator is able to switch to either method as the need arises. Therefore, this docking method applies the merits of both teleoperation and autonomous control, and the robot is able to connect to the wheelchair without a high-performance sensor system. In this paper, we discuss the connecting system, the procedure of docking the vehicles, and the theoretical analysis to connect the vehicles by using dual manipulators of the robot. The experimental results show the effectiveness of this method.**

***Index Terms*—docking, wheelchair, robot, connecting, step climbing**

I. Introduction

Most wheelchairs have wheel mechanisms, and they are able to move easily on a flat road. However, one of their weaknesses is the inability to overcome steps. Many studies have improved wheelchair mobility on steps by mounting additional legs [1], using the combination of an adjustable center of gravity and multiple wheels [2], and using the wheelchair posture to climb [3]. In addition to step climbing, wheelchair users have to perform many difficult tasks in their daily life (opening a door, picking up an object, etc.). The research group of the present report has studied a care robot which is able to remove such difficulties for wheelchair users, and they have presented the cooperative step climbing method for a wheelchair and a robot (Fig. 1) [4]. These vehicles are deployed in a forward-and-aft configuration before step climbing.

Either an autonomous robot or a teleoperated robot can find and connect with another vehicle, and each type of robot has its own merits. The wheelchair and partner robot have individually driven wheels, and the trajectories of both vehicles are limited. When both vehicles move at the same time, it is difficult to connect them because the relative distance between the two vehicles can change suddenly. Thus, it is desirable to stop one of the vehicles to connect them.

In general, when an autonomous robot is comparatively distant from another vehicle and does not know the position of either itself or the other vehicle, the robot needs a high-performance sensor system to connect with the other vehicle. However, when an autonomous robot is next to the other vehicle, it is not too difficult to connect with the other vehicle, even without a high-performance sensor system. Alternatively, when a robot operator controls a teleoperated robot which has individually driven wheels, it can be difficult to exactly connect with the other vehicle because the trajectory of the robot is limited. However, it is not difficult for the robot operator to control the teleoperated robot to find the other vehicle or to give the teleoperated robot access to it even if the operator does not know the position of the other vehicle [5]. The present report describes the docking method for the wheelchair and the care robot that uses both teleoperation and autonomous control. Many studies of the connecting method between a wheeled robot and another independent system have reported, for example, docking to battery charging systems using a wheeled robot with a flexible joint mechanism [6], using lamps as active markers [7], and connecting tracked vehicles which have special docking grippers [8].

Based on preliminary measurements of friction coefficients of the robot in wet and dry conditions on asphalt, concrete, wood, and interior flooring, the ground surface considered in this research was assumed to have a friction coefficient in the range of 0.6 to 0.9, which is satisfactory for all of the above wet and dry conditions.

This paper is organized as follows. Section II describes the system and the cooperative step climbing process for the wheelchair and the robot. Section III describes the connecting process with the wheelchair and the robot and an analysis to connect the vehicles. Section IV presents

Manuscript received July 13, 2015; revised December 26, 2015.

doi: 10.18178/ijmerr.5.2.82-89

the experimental setup and experimental results, and Section V is the conclusion.

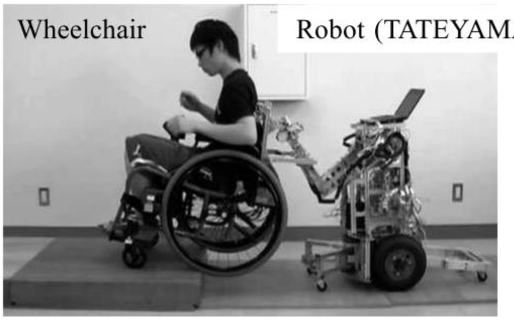

Figure 1. Wheelchair and robot

TABLE I. SPECIFICATIONS OF THE ROBOT

Overall length	230 to 800 [mm]
Overall height	747 [mm]
Radius of front wheels (r_{Bf})	25 [mm]
Radius of middle wheels (R_B)	145 [mm]
Radius of rear wheels (r_{Br})	19 [mm]
Wheelbase (WB_f)	190 to 440 [mm]
Wheelbase (WB_r)	270 [mm]
Distance of center of mass from the middle wheel axes (l_{rB})	93 [mm]
Height of the mass above the center wheel axes (h_{mB})	286 [mm]
Distance of Joint 2 from the rear axes (l_{LB})	90 [mm]
Height of Joint 2 above the rear axes (h_{LB})	532 [mm]
Mass of the robot body	55 [kg]
Mass of Link 2 (from Joints 2 to 4)	2.55 ×2 [kg]
Mass of Link 4 (from Joint 4 to hand)	0.8 ×2 [kg]
Length of Link 2 (l_2)	330 [mm]
Length of Link 4 (l_4)	300 [mm]
Length of the hand (l_6)	105 [mm]
Length from Joint 4 to the connecting position (l_{4c})	370 [mm]
Center of mass position of Link 2 (L_2)	67 [mm]
Center of mass position of Link 4 (L_4)	169 [mm]
Center of mass position of Link 6 (hand mechanism) (L_6)	35 [mm]
Distance between the right and left hands d	360 [mm]

II. WHEELCHAIR AND ROBOT

The robot used in this research was the wheeled "TATEYAMA" developed in this laboratory [4] (Fig. 1). Table I provides the specifications of the robot. In climbing or descending a step, the robot connects to the wheelchair (Fig. 2). The robot has three left/right wheel pairs. The front and rear pairs are casters that can be shifted into different positions, and the middle pair are driving wheels. Fig. 3 shows the manipulator of the robot; the robot has dual manipulators attached to the left and right sides of the upper half of its body. In addition to the 5 degrees of freedom (DOF) on the arm, the hand has 1 DOF for a total of 6 DOF. In this study, the link from Joint 2 (shoulder) to Joint 4 (elbow) is called "Link 2" (length l_2), that from Joint 4 to Joint 5 (wrist) is called "Link 4" (length l_4), and that from Joint 5 to the tip of the hand is called "Link 6" (length l_6). The length from the elbow, Joint 4 to Joint 6 (the location of the connection between the wheelchair and the robot), is designated l_{4c}. As shown in Fig. 2, the manipulator joint angles are -90 [deg] $\leqslant \emptyset_2 \leqslant$+90 [deg] and 0 [deg] $\leqslant \emptyset_4 \leqslant$ +100 [deg]. The left and right hands each have two fingers for grasping objects (Fig. 4). These fingers have springs and touch sensors that are covered by bumpers (Bumpers A, B) connected to the fingers by hinges. The touch sensors on these fingers are able to detect grasping of the wheelchair shaft (Fig. 5). Both hand mechanisms have another touch sensor (Bumper C) between the two fingers. This touch sensor is able to detect the contact with the wheelchair shaft when the robot connects to the wheelchair. The robot has a stopper mounted on its front as a part of its body (Fig. 6 (a)). This enables the robot to imitate the operation in which a human pushes an object by limiting the passive rotation about the shoulder joint as the upper arm is pushed into the chest (Fig. 6 (b)). As described below, the robot stopper limits the passive rotational travel of the manipulators when the robot has been pushed (Fig. 7). The robot has a camera (Fig. 8), and its shooting angle is controlled by the robot operator via an intranet.

TABLE II. SPECIFICATIONS OF THE WHEELCHAIR

Overall length	1060 [mm]
Overall height	985 [mm]
Radius of front wheels (r_A)	63 [mm]
Radius of rear wheels (R_A)	300 [mm]
Wheelbase (l_A)	430 [mm]
Handrim position (l_{LA})	250 [mm]
Distance of center of mass from the rear wheel axes (l_{rA})	149 [mm]
Height of mass above the rear wheel axes (h_{mA})	371 [mm]
Length of the shaft (l_s)	520 [mm]
Mass (wheelchair + driver) (M_A)	92.7 [kg]

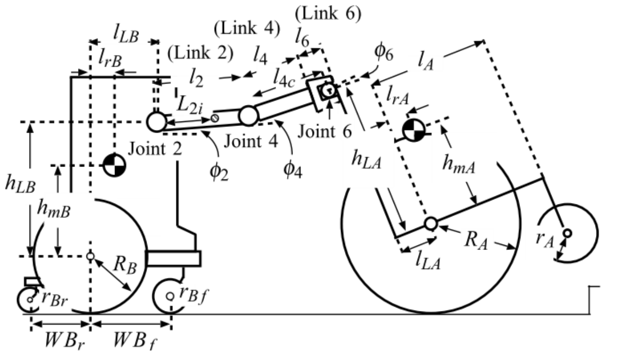

Figure 2. Model of the wheelchair and the robot

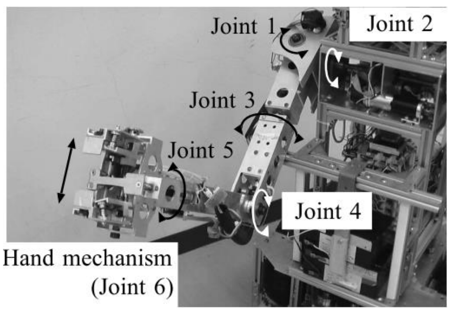

Figure 3. Manipulator of the robot.

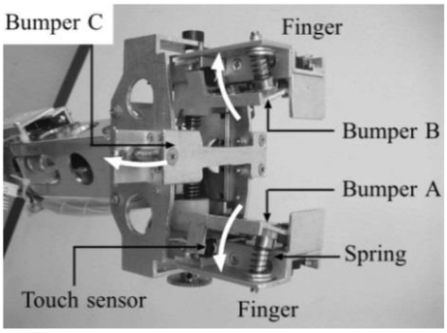

Figure 4. Hand mechanism

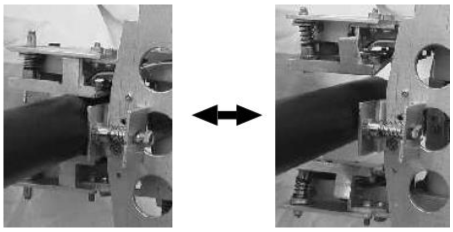

Figure 5. Grasping and releasing the shaft

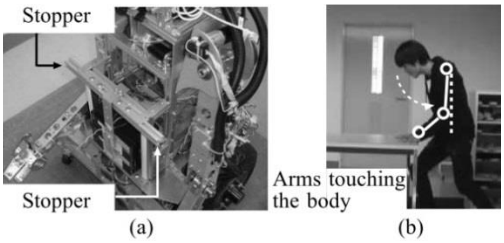

Figure 6. Control of rotary motions of the robot shoulder by using the body. (a) Front body of the robot. (b) Human pushing an object

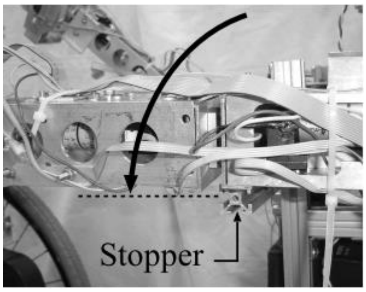

Figure 7. Side view of stopper on the robot chest

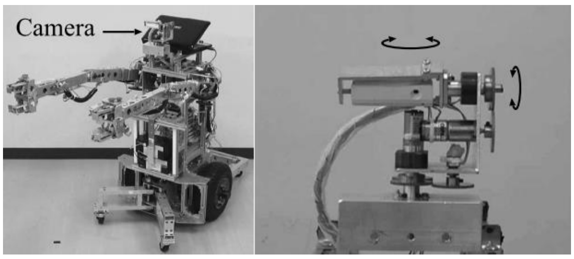

Figure 8. Camera on the robot

The wheelchair (NOVA Integral-ME) used in the experiment has a shape typical of wheelchairs available on the market (Fig. 1). Table II provides specifications of the chair. The chair was rear-wheel drive, and it had a push handle mechanism on the back for the robot hands to grasp (Figs. 9 (a) and (b)). The push handle mechanism was equipped with a rotary shaft which allowed passive rotation of the handle, and the surface was rubberized.

The robot hands grasped this shaft and thus connected to the wheelchair. The angle formed by the wheelchair with Link 4 was Ø_6 (Fig. 2). The wheelchair stopper, composed of the front and rear bars (Figs. 9 (a) and (b)), is mounted on the rear side. During climbing and descending of the robot, the left and right sides of the robot are opened, and the two manipulators are inserted into the stopper (Fig. 9 (a)). The robot pushes the front bars to lift the front wheels of the robot. The rear bars prevent the robot from tipping over backward when the robot mass position shifts behind the contact point between the center wheels and the ground (Fig. 9 (b)).

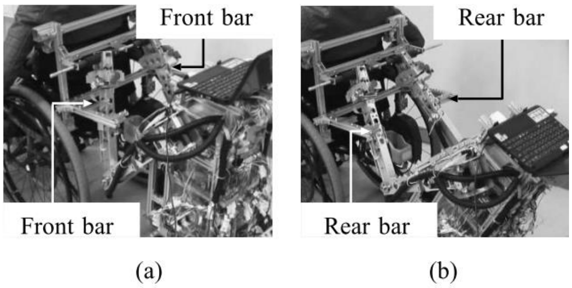

Figure 9. Action of the wheelchair stopper. (a) Position of bar to lift the front wheels of the robot. (b) Position of bar to prevent the robot from tipping over by using the wheelchair stopper.

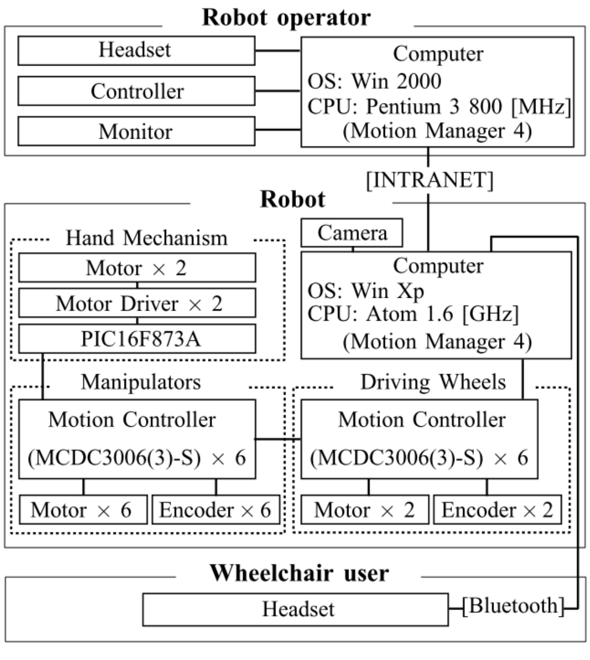

Figure 10. Diagram of the system (teleoperating robot mode)

Fig. 10 is a system configuration diagram. The teleoperated robot was operated by a robot operator (caregiver). In this study, the robot control mode can be switched between teleoperation to autonomous control by the robot operator (caregiver). The motors mounted on the robot were connected to Faulhaber motion controllers (Faulhaber MCDC3006-S, MCDC3003-S). In turn, these were connected to a notebook PC mounted on the robot. The motors were controlled via commands issued by the

Motion Manager 4 software package. The moving images from the camera on the robot (Fig. 8) and the Motion Manager 4 operating window were displayed on the notebook PC mounted on the robot. The screen on this notebook PC used Real VNC software and was transmitted over the intranet as-is to the display of a PC used by the robot operator at a different location. The robot operator was able to control the robot by operating Motion Manager 4 from his PC. The commands for Motion Manager 4 were issued by JoyToKey software.

The keyboard commands, which were activated by pushing the buttons of the Joypad, corresponded to the manipulation of the controller to operate the robot. The robot controller (caregiver) and the wheelchair user both wore headsets and used the telecommunication software Skype to communicate verbally. The caregiver's headset was connected to the caregiver's PC, and the wheelchair user's headset was connected to the PC on the robot.

In this study, the robot was operated at a constant speed (0.76 [km/h]).

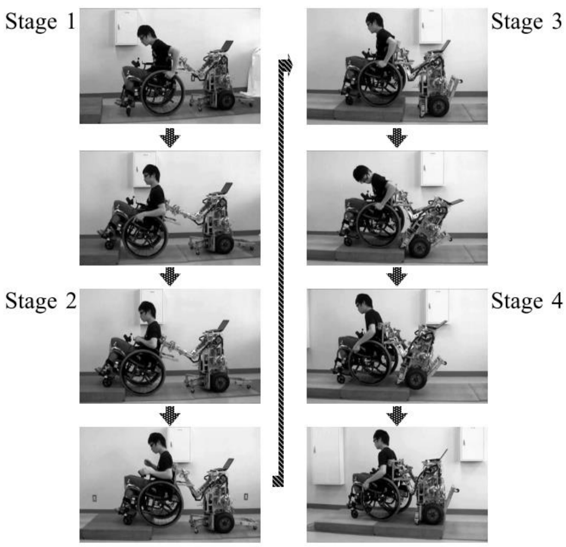

Figure 11. Cooperative step climbing

The research group of the present report previously achieved cooperative step climbing for a wheelchair and a wheeled robot [4]. The step climbing method is divided into four processes (stages 1 - 4). The first two stages describe the wheelchair actions, and the second two stages describe the robot actions. Stage 1 and stage 2 signify the processes in which the front and the back wheels of the wheelchair, in that order, ascend the step. Similarly, stage 3 and stage 4 signify the processes in which the front and the back wheels of the robot, in that order, ascend the step (Fig. 11). These step climbing processes are described below.

[Stage 1]

Joints 2, 4, and 6 (Fig. 3) are allowed to rotate passively until the ascent of the wheelchair has been completed. The robot operator (caregiver) stops the robot. The wheelchair user manipulates the handrims, as if to move forward, to lift the front wheels. If the wheelchair center of gravity shifts behind the contact point between the back wheels and the ground as the wheelchair tilt increases, the chair exerts forces on the manipulators and causes passive rotation about Joint 2. In this case, the manipulator upper-arm link comes into contact with the robot stopper and limits the extent of the rotation (Fig. 7).

The robot moves forward and the wheelchair user manipulates the handrims to adjust the difference between the speeds of the two vehicles, so that the front wheels of the wheelchair are placed on the upper level of the step.

[Stage 2]

The robot continues to move forward while pushing the wheelchair from behind. The back wheels of the wheelchair come into contact with the step. The robot continues to push on the wheelchair so that the rear wheels of the wheelchair climb up the step. The robot supports the wheelchair during this process to prevent the wheelchair from tipping over backward. Once the wheelchair rear wheels have reached the upper level of the step, the robot stops.

[Stage 3]

The front and rear wheels of the robot are folded into/against the robot body. The right and left sides of the robot are opened, and the two manipulators are inserted in the wheelchair stopper (Fig. 9 (a)). The wheelchair user maintains the wheelchair position. The robot moves forward, bringing the manipulator forearm link into contact with the stopper (front bars) of the wheelchair. The robot continues to move forward. The front wheels of the robot are lifted (Fig. 9 (a)). When the robot center of mass shifts behind the contact point between the middle wheels, part of the manipulator forearm link comes into contact with the wheelchair stopper (rear bars) and limits the extent of rotation (Fig. 9 (b)). The robot and the wheelchair move forward. The front wheels of the robot are placed on the upper level of the step.

[Stage 4]

Both vehicles move forward, and the middle wheels of the robot come into contact with the step. The wheelchair pulls the robot, the robot is able to avoid tipping over, and the middle wheels of the robot start to climb the step. Both vehicles continue to move forward. The middle wheels of the robot are able to climb the step. After the middle wheels have reached the upper level of the step, both vehicles stop.

III. METHOD OF CONNECTING THE VEHICLES

By teleoperation using the camera on the robot, it is comparatively easy to enable the robot to access the wheelchair roughly from an area detached from the wheelchair. Alternatively, by autonomous control of the robot, it is also comparatively easy to exactly connect to the wheelchair when the robot is in the immediate area of the wheelchair. The connecting method proposed in this paper uses the merits of both teleoperation and autonomous control.

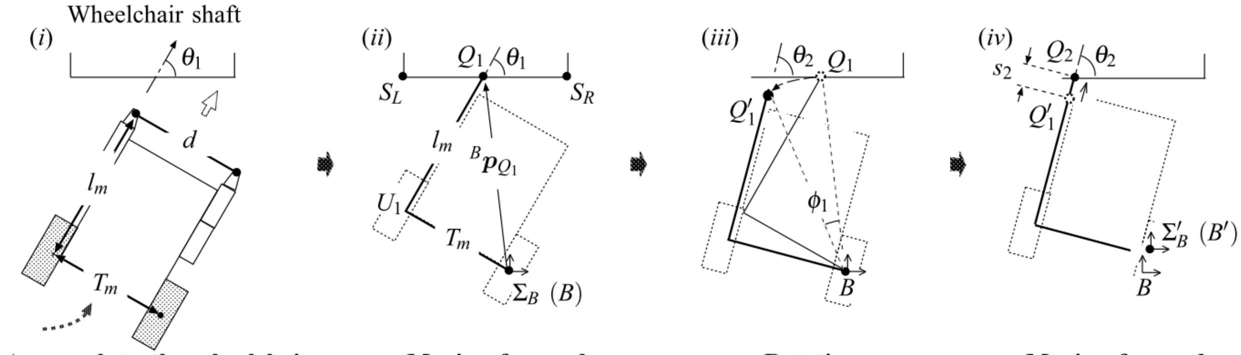

Figure 12. Process of dockin

A. Process of Connection

In this paper, we illustrate the docking process when the left robot hand first makes contact with the wheelchair shaft. The robot operator considered in the present study was assumed to know the height of the wheelchair shaft, and we assume that the wheelchair and the robot are on a flat road during the connecting.

θ_1 is the first angle formed by the shaft of the wheelchair and the robot posture (Fig. 12 (*1*)). $\sum_B$ is the basic coordinate system for the robot, where contact point B is between the robot right middle (driving) wheel and the ground is the origin. Q_1 is the first contact point between the wheelchair shaft and the left robot hand (Fig. 12 (*2*)), S_L is the left edge position of the wheelchair shaft, S_R is the right edge position of the wheelchair shaft, U_1 is the point of intersection formed by the line of the middle wheels' axes and the straight line from Q_1 to the rear of the robot. T_m is the length from point B to U_1 , l_m is the length from Q_1 to U_1, and d is the distance between the left and right robot hands.

1) Teleoperation for giving the robot access to the wheelchair

First, the operator teleoperates the robot hand to be at the same height of the wheelchair shaft. Next, the robot operator teleoperates the robot camera to find the wheelchair. Then, the robot operator teleoperates the robot toward the center of the wheelchair shaft and beside position as he can (Fig. 13).

Figure 13. Approach to the wheelchair by the teleoperated robot.

2) Switching over from teleoperation to autonomous control, and first contact with the wheelchair shaft

The operator switches over from teleoperation to autonomous control by using the controller. The operator pushes the controller button, and then the robot starts to move forward. The robot keeps moving by autonomous control until the end of the connecting process. If the left and right hands of the robot touch the shaft at the same time, the robot stops and both hands grasp the shaft, and the wheelchair and the robot finish the connecting process. If the connecting process is not accomplished, the robot is controlled by the rule of the next process.

3) Rotation

The middle wheel on the opposite side where the hand touched the shaft (in Fig. 12, the right middle wheel) remains stopped and the same side middle wheel (in Fig. 12 (*3*), the left middle wheel) drives backward as the hand leaves the shaft. (The robot rotates until the hand leaves the wheelchair shaft.) The ingress angle is changed from θ_1 to θ_2, and the left hand position is changed from Q_1 to $Q_1{}'$.

4) Moving forward, and second contact with the wheelchair shaft

The robot moves forward (the distance is s_2) by the left hand contact with the wheelchair shaft (Fig. 12 (*4*)).

Thus, the left hand position is changed from $Q_1{}'$ to Q_2, and the contact point of the right middle wheel and the ground is changed from B to B'. If the right and left hands contact the shaft at the same time, the robot stops and both hands grasp the shaft. The wheelchair and the robot finish the connecting process. If the connecting process is not complete, the robot is controlled *b*y the rule of "(*3*) Rotation."

The robot repeats the rotation and the moving forward, and the ingress angle (θ_n) is approximately 90 [deg]. Thus, both robot hands are able to grasp the wheelchair shaft.

B. Requirement for Connecting when Both hands Grasp the Shaft

In this connecting method, the robot has to grasp the wheelchair shaft with the right and left robot hands. This docking method repeats the moving forward and rotation of the robot, and the grasping position Q_n leaves the first contact point Q_1. When the position and the ingress angle of the robot are greatly different from the wheelchair, the case in which the right or left hand is not able to grasp the shaft may occur (Fig. 14).

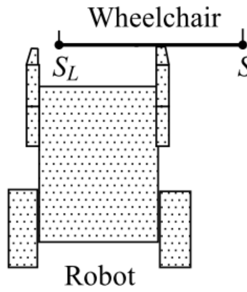

Fiure 14. Case of one hand not being able to grasp the shaft

In this section, we analyze the range of the first contact position (Q_1), in which both robot hands are able to grasp the shaft. Fig. 15 shows the state that the left hand first contacts the wheelchair shaft, and the state that both hands grasp the shaft. The distance between the right hand and the left hand is constant (= d). l_s is the length of the wheelchair shaft, and k ($0 \leq k \leq 1$) is the coefficient of the relationship between the total length of the shaft and the first contact position (Q_1). Thus, the length from S_L to Q_1 is $k \cdot l_s$ (Fig. 15).

The position vectors for the left tip of the shaft (${}^{B}\boldsymbol{p}_{S_L}$) and the right tip (${}^{B}\boldsymbol{p}_{S_R}$) of the shaft are expressed as

$${}^{B}\boldsymbol{p}_{S_L} = [l_m \cos\theta_1 - T_m \sin\theta_1 - kl_s \quad l_m \sin\theta_1 + T_m \cos\theta_1]^{T} \quad (1)$$

$${}^{B}\boldsymbol{p}_{S_R} = [l_m \cos\theta_1 - T_m \sin\theta_1 + (1-k)l_s \quad l_m \sin\theta_1 + T_m \cos\theta_1]^{T} \quad (2)$$

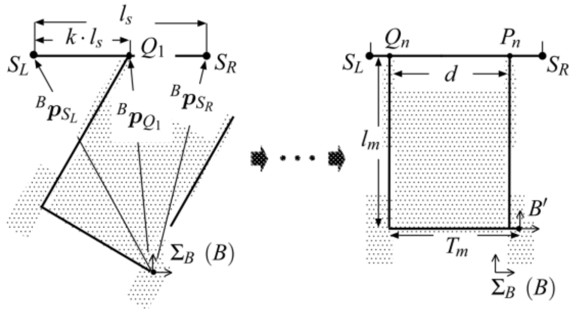

Figure 15. Difference between primary contact position and final position (connecting position)

The robot repeats both moving forward and the rotation to approximate the ingress angle (θ_1) to 90 [deg]. When the hands grasp the shaft after moving forward n times, the left hand position, 〖(_^B)p〗_(Q_n)=Q_n 〖[x_qn y_qn]〗^T, is given bytence, as in

$${}^{B}\boldsymbol{p}_{Q_n} : \begin{bmatrix} x_{qn} \\ y_{qn} \end{bmatrix} = \begin{bmatrix} \cos(\theta_1 + \sum \emptyset_{n-1}) & -\sin(\theta_1 + \sum \emptyset_{n-1}) \\ \sin(\theta_1 + \sum \emptyset_{n-1}) & \cos(\theta_1 + \sum \emptyset_{n-1}) \end{bmatrix} \begin{bmatrix} l_m \\ T_m \end{bmatrix} + \begin{bmatrix} \sum s_n \cos\theta_n \\ \sum s_n \sin\theta_n \end{bmatrix} \quad (3)$$

Here, $\emptyset_0 = 0$, $s_1 = 0$.

The distance between the right and left hands is d, and thus the right hand position, 〖(_^B)p〗_(P_n)=P_n 〖[x_pn y_pn]〗^T, is given by

$${}^{B}\boldsymbol{p}_{P_n} : \begin{bmatrix} x_{pn} \\ y_{pn} \end{bmatrix} = \begin{bmatrix} \cos(\theta_1 + \sum \emptyset_{n-1}) & -\sin(\theta_1 + \sum \emptyset_{n-1}) \\ \sin(\theta_1 + \sum \emptyset_{n-1}) & \cos(\theta_1 + \sum \emptyset_{n-1}) \end{bmatrix} \begin{bmatrix} l_m \\ T_m \end{bmatrix} + \begin{bmatrix} \sum s_n \cos\theta_n \\ \sum s_n \sin\theta_n \end{bmatrix} + \begin{bmatrix} d \\ 0 \end{bmatrix} \quad (4)$$

In connecting both vehicles, $\theta_1 + \sum \emptyset_{n-1} = 90$ [deg], and so ${}^{B}\boldsymbol{p}_{Q_n}$ and ${}^{B}\boldsymbol{p}_{P_n}$ are expressed as

$${}^{B}\boldsymbol{p}_{Q_n} : \begin{bmatrix} x_{qn} \\ y_{qn} \end{bmatrix} = \begin{bmatrix} -T_m + \sum s_n \cos\theta_n \\ l_m + \sum s_n \sin\theta_n \end{bmatrix} \quad (5)$$

$${}^{B}\boldsymbol{p}_{P_n} : \begin{bmatrix} x_{pn} \\ y_{pn} \end{bmatrix} = \begin{bmatrix} -T_m + \sum s_n \cos\theta_n + d \\ l_m + \sum s_n \sin\theta_n \end{bmatrix} \quad (6)$$

From the x coordinates of (1) and (5), we obtain equation (7), which is the requirement to enable the left hand to grasp the shaft.

$$l_m \cos\theta_1 - T_m \sin\theta_1 - kl_s < -T_m + \sum s_n \cos\theta_n \quad (7)$$

Similarly, we obtain equation (8) from the x coordinates of (2) and (6), which is the requirement to enable the right hand to grasp the shaft

$$l_m \cos\theta_1 - T_m \sin\theta_1 + (1-k)l_s > -T_m + \sum s_n \cos\theta_n + d \quad (8)$$

From (7) and (8), we obtain (9), which is the requirement that enables both hands to grasp the shaft.

$$\frac{e_1}{l_s} \leq k \leq 1 + \frac{e_1 - d}{l_s} \quad (9)$$

here, $e_1 = l_m \cos\theta_1 + T_m(1 - \sin\theta_1) - \sum s_n \cos\theta_n$, and s_n is the distance between detecting the contact with the shaft and leaving it (3 [mm], Fig. 4).

If $\theta_1$is close to 90 [deg], then n is small in this system, and we can assume $\sum s_n \cos\theta_n \approx 0$ in (9).

IV. EXPERIMENT

An experiment was carried out with this system in an environment with a flat load of the friction coefficient, μ=0.64. The wheelchair user and the robot operator were both able-bodied adult males. The robot operator performed his task over a network while observing the situation via the camera and communicating with the wheelchair user over a voice link by using Skype. The wheelchair user was on one floor of the National Institute of Technology, Toyama College, and the robot operator was in another building of this college. The robot speed was constant (0.76 [km/h]), and l_m= 0.788 [m], T_m= 0.37 [m] in this experiment (Fig. 12). Fig. 16 shows the arrangement of the vehicles. In this experiment, the robot operator does not know the wheelchair position at the beginning of the experiment.

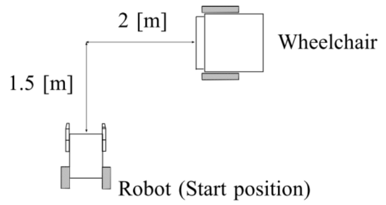

Figure 16. Relationship of the vehicle positions in the experiment

In the teleoperating process, the robot operator makes the robot access the rear of the wheelchair and matches the position of the center of the shaft as much as possible. The operator controls the robot ingress angle to the wheelchair (θ_1) to be 90 [deg]. However, the robot operator must not turn the wheels to correct the position in the experiment.

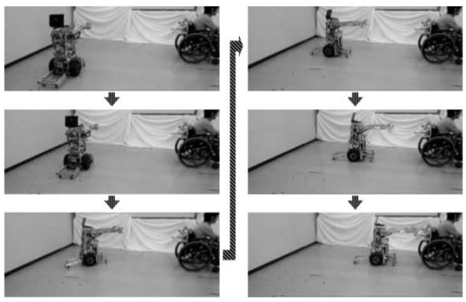

Figure 17. Experiment: Teleoperation for approaching the wheelchair

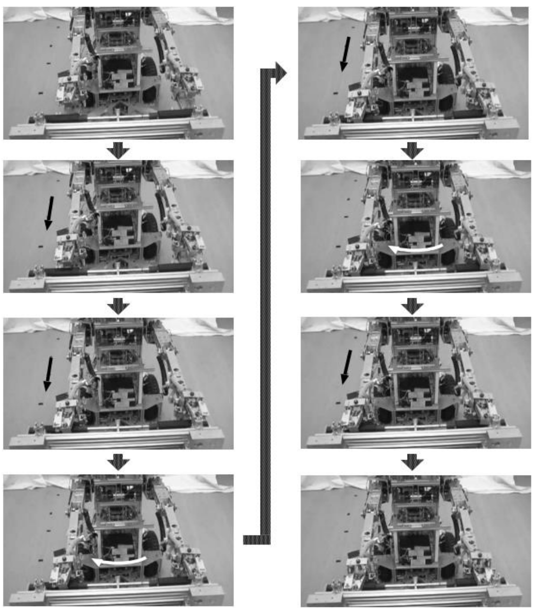

Figure 18. Experiment: Autonomous control for grasping the wheelchair shaft.

As the result of the experiment, the robot operator was able to find the wheelchair by using the camera on the robot, and the operator was also successful in making the robot access the rear of the wheelchair without turning the wheels (Fig. 17). Then, the operator changed from teleoperation to autonomous control and the robot moved forward. The robot hand contacted the wheelchair shaft, and repeated moving forward and turning 3 times, and both robot hands were able to grasp the wheelchair shaft (Fig. 18).

Other subjects (4 adult males) tried the same operation. As the results of the experiments, the differences from the vehicle centers were within ±50 [mm], and the ingress angles were 85 [deg] $\leq \theta_1 \leq$ 95 [deg] when the robot first contacted the wheelchair shaft. After repeating the moving forward and the rotation operations, the subjects were able to make the robot grasp the shaft with both hands.

V. CONCLUSION

This paper describes a docking method for a wheelchair and a caregiver robot that uses teleoperation or autonomous control. We constructed the system, and the theoretical analysis shows the requirement by which both hands could grasp the wheelchair shaft. We carried out experiments incorporating teleoperation of the robot over an intranet, and these connecting tactics were demonstrated to be effective. In the future, we will construct a system for supporting the operation to connect, and analyze a suitable trajectory for the robot to connect with the wheelchair.

REFERENCES

[1] V. Kumar and V. Krovi, “Optimal traction control in a wheelchair with legs and wheels,” in *Proc. 4th National Applied Mechanisms and Robotics Conference*, 1995, pp. 95-030-01-95-030-07.

[2] iBOT. Segway Inc.'s Human Transporter (HT) Models. [Online]. Available: http://msu.edu/~luckie/segway/iBOT/iBOT.html.

[3] M. Lawn and T. Ishimatsu, “Modeling of a stair-climbing wheelchair mechanism with high single step capability,” *IEEE Trans. on Neural Systems and Engineering*, vol. 11, no. 3, pp. 323-332, 2003.

[4] H. Ikeda, H. Kanda, N. Yamashima, and E. Nakano, “Step climbing and descending for a manual wheelchair with a network care robot,” in *Proc. 2nd International Conference on Intelligent System and Applications*, 2013, pp. 95-102.

[5] N. Yamashima and H. Ikeda, “Experiments of connection between a wheelchair and a care robot which is worked by fusion of teleoperation through an intranet and autonomous control,” *Robomech 2012 in Japan*, 2A1-G04, 2012.

[6] M. C. Silverman, D. Nies, B. Jung, and G. S. Sukhatme, “Staying alive: Docking station for autonomous robot recharging,” in *Proc. IEEE International Conference on Robotics and Automation*, 2002, pp. 1050-1055.

[7] R. Cassinis, F. Tampalini, P. Bartolini, and R. Fedrigotti, “Docking and charging system for autonomous mobile robot,” Department of Electronics for Automation, University of Brescia, Italy, 2005.

[8] W. Wang, W. Yu, and H. Zhang, “JL-2: A mobile multi-robot system with docking and manipulating capabilities,” *International Journal of Advanced Robotics Systems*, vol. 7, no. 1, pp. 9-18, 2010.

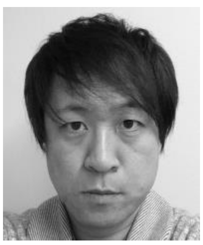

Hidetoshi Ikeda received his MS degree (1999) and PhD (2002) in Information Sciences from Tohoku University, Japan. He joined Sanyo Corp. from 2002 to 2004. From 2004 to 2008, he was Assistant Professor at Toyama National College of Technology. Since April 2008, he has been Associate Professor. Dr. Ikeda is a member of the Robotics Society of Japan, IEEE Robotics and Automation Society.

Nobuyuki Yamashima graduated the Department of Mechanical Engineering, Toyama National College of Technology, in 2011. From 2011 to 2013, he was student of Advanced Engineering Faculty in this college. He was student of Graduate school of Ibaragi University from 2013 to 2015, and received his MS degree.

Shogo Haruta graduated the Department of Mechanical Engineering, Toyama National College of Technology, in 2009. From 2009, he was student of Nagoya Institute of Technology and received his B.Tc degree in 2011. He is student of Graduate school of National Defense Academy, Japan.

Eiji Nakano was Graduated, Postgraduate Course of University of Tokyo in 1970, Senior Researcher, Mechanical Engineering Laboratory in 1970. Professor, Tohoku Unive